Title

Overpotential-derived thermogenesis in mitochondrial respiratory chain

Authors

Nuning Anugrah Putri Namari[1], Mo Yan[1], Junji Nakamura*[2,3 §], Kotaro Takeyasu*[2,3,4]

Affiliations

[1] Graduate School of Science and Technology, University of Tsukuba; 1-1-1 Tennodai, Tsukuba, Ibaraki 305-8573, Japan.

[2] Department of Materials Science, Faculty of Pure and Applied Sciences, University of Tsukuba; 1-1-1 Tennodai, Tsukuba, Ibaraki 305-8573, Japan.

[3] Tsukuba Research Centre for Energy and Materials Science, University of Tsukuba; 1-1-1 Tennodai, Tsukuba, Ibaraki 305-8573, Japan.

[4] R&D Center for Zero CO_2 Emission with Functional Materials, University of Tsukuba; 1-1-1 Tennodai, Tsukuba, Ibaraki 305-8573, Japan.

[§] Current address: International Institute for Carbon-Neutral Energy Research (I^2CNER), Kyushu University; 744 Motooka, Nishi-ku, Fukuoka-shi, Fukuoka 819-0395, Japan.

Thermogenesis, which is associated with intracellular aerobic respiration, is a fundamental function that controls the internal temperatures of living organisms. Proton leakage is considered to be correlated with thermogenesis through aerobic respiration. It is widely known that in electrochemical cells such as fuel cells, overpotentials applied to redox reactions generate heat as energy loss. Even in the electrochemical reaction system of the mitochondrial respiratory chain, a considerable amount of heat is generated by overpotential. However, the physical mechanism of thermogenesis is not yet clear. We propose a thermogenesis model based on the electrochemical overpotential of the mitochondrial respiratory chain. As a result of quantitatively estimating the value of the overpotential applied in each reaction of the mitochondrial respiratory chain, we found that 39-63% of the initial free energy in the respiratory chain was converted into heat, and the rate of thermogenesis changed depending on respiratory activity. Furthermore, that heat was intensively produced in complex IV. The overpotential-derived thermogenesis model is expected to open a research field for electrochemically elucidating mitochondrial functions.

Main text

Intracellular thermogenesis is one of the most basic biological processes required to sustain life[1–5]. However, the physical mechanism of the thermogenesis has not yet been clarified experimentally or theoretically. The widely accepted theory that thermogenesis originates from proton leakage across the inner mitochondrial membrane has little experimental or theoretical basis[5–7]. However, energy loss (overpotential) in the electrochemical reaction that proceeds like a fuel cell in the mitochondrial respiratory chain is likely the cause of thermogenesis. In enzyme complexes I–IV in the respiratory chain, electrons flow constantly from the oxidation of NADH

to the reduction of oxygen molecules. Each enzyme generates heat because redox reactions require an overpotential. The oxygen reduction reaction in the respiratory chain is similar to that in fuel cells, where the overpotentials are converted to heat corresponding to electrical energy loss (see Fig. 1a, b, c). Research on the mitochondrial respiratory chain reaction as a fuel cell system was conducted by Bockris[8,9] and Berry[10] in the 1980s. However, the detailed structure of the respiratory chain was unknown, and Mitchell's chemiosmosis hypothesis[11,12] became widespread. However, electrochemical reactions accompanied by fuel cell-like overpotentials occur in the mitochondrial respiratory chain, and it is necessary to re-examine the thermogenesis mechanism derived from the overpotential. The oxygen reduction reaction at the fuel cell cathode requires an overpotential of 0.3 V or more to drive the reaction, even if the most advanced platinum-based catalyst is used, and after the reaction is driven, it is dissipated as Joule heat.

The theoretical treatment of fuel cell models can be regarded as an analysis of nonequilibrium phenomena. In other words, it is not about dividing the free energy change of a reaction based on simple thermodynamics, because the analysis of thermogenesis is related to the reaction kinetics at the steady state, which corresponds to non-equilibrium thermodynamic theory. In this paper, we propose an "overpotential-derived electrochemical thermogenesis model" in which an electrochemical driving force or Gibbs free energy drop is used as an overpotential to drive a reaction and is then dissipated as heat. Electrocatalytic reactions at the steady state when an overpotential is applied are kinetic or non-equilibrium phenomena, and the generation of heat is non-equilibrium energetics. In other words, the thermogenesis is related to the reaction rate. In the field of chemical reactions, it is generally understood that most of the energy used during a reaction is distributed during the rate-determining process. The above discussion also applies to redox reaction systems in living organisms. The basic principles of the non-equilibrium theory of reactions in living organisms have been developed by Prigogine, Kacharski, and others[9]. However, considering that energy transfer based on specific biological reaction systems remains a major problem, it is also a way to elucidate the physics of life phenomena.

In this study, we verified that the majority of thermogenesis in the mitochondrial respiratory chain is derived from the overpotential. Furthermore, we verified that the energy balance between overpotential-induced thermogenesis and ATP production is modulated by the reaction rate of the respiratory chain, that is, respiratory activity. Specifically, we used literature data from electrochemical experiments in our proposed overpotential-thermogenesis model to estimate the amount of thermogenesis, and the calculated ratio of thermogenesis relative to the Gibbs free energy of oxygen reduction reaction was compared with the generally reported ratio of thermogenesis (40–60 %)[13,14]. We also clarify whether it is necessary to consider frictional heat due to proton movement within the membrane. Electrochemical experimental data are now available regarding the enzymatic reaction system of the mitochondrial respiratory chain. Therefore, it is possible to discuss the magnitude of the overpotential at any current value and the thermogenesis derived from the overpotential. In this study, we estimated the relationship between the overpotential and current for the steady state of respiratory chains I, III, and IV, and estimated the sum of the total overpotential at a certain current value by considering the

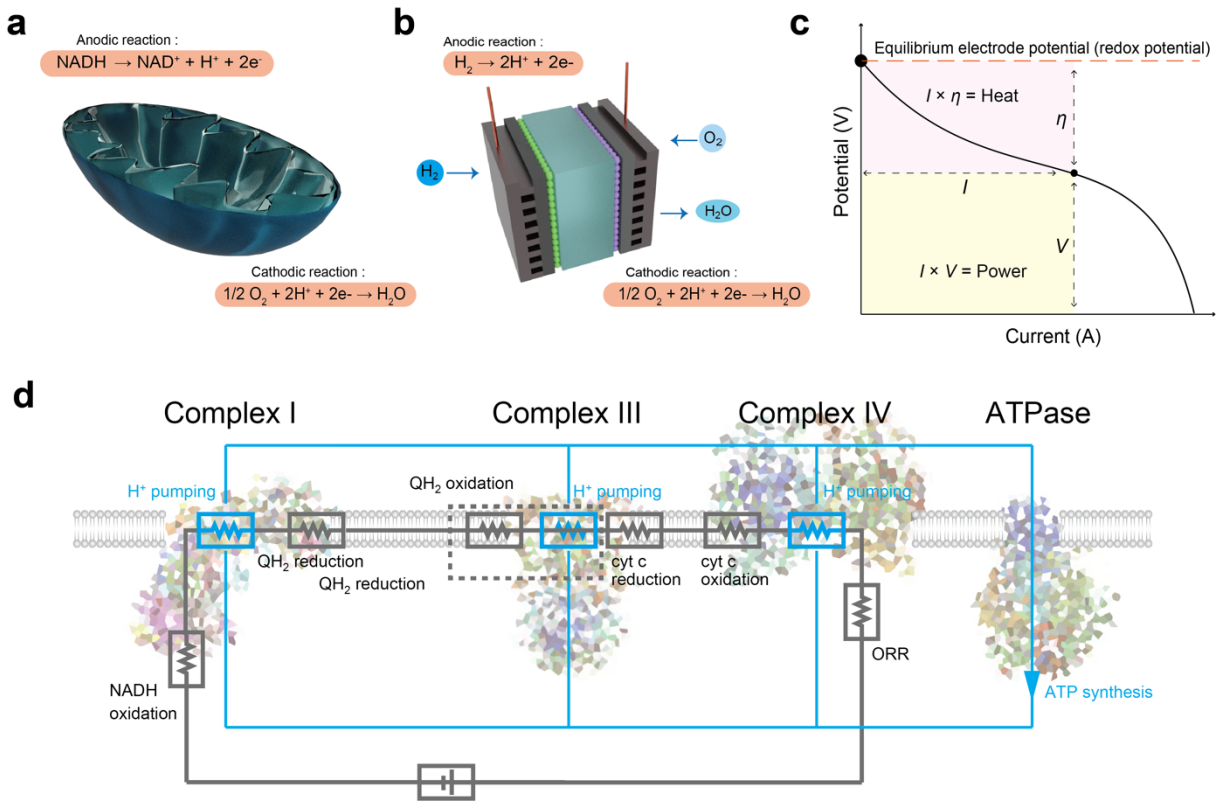

Fig. 1 | Thermogenesis model based on the electrochemical overpotential of the mitochondrial respiratory chain. Analogy of reactions in **a,** mitochondrial respiratory chain and **b**, hydrogen fuel cell. **c**, typical voltage-current curve for hydrogen fuel cell. The overpotential applied to drive the reaction is converted to heat. **d**, Reaction circuit model of a mitochondrial respiratory chain.

series circuit shown in Fig. 1d. This determines the relationship between the current and the sum of the overpotentials. Furthermore, the current and overpotential values were converted numerically into respiration rate and heat, respectively.

First, it is necessary to understand the electrochemical properties of enzymes in the respiratory chain, that is, the relationship between current j and overpotential η including the transmission coefficient α. As shown in equation (1), the relationship among η, j, α, and exchange current value j_0 follows the Butler-Volmer equation, so if α and j_0 are known, the relational expression between η and j can be derived. By substituting the current value j in the steady state into the derived equation, the overpotential η can be estimated.

$$j = j_0 \left\{ e^{\frac{(1-\alpha)zF}{RT}\eta} - e^{-\frac{\alpha zF}{RT}\eta} \right\} \quad (1)$$

In this study, α and j_0 in complexes I, III, and IV were estimated from literature data[15–26]. That is, α and j_0 were determined by fitting the voltammogram measured for the enzyme or

enzyme model system. Specifically, for the linear sweep voltammogram, a simulation was performed using the Butler-Volmer equation (1), and for the cyclic voltammogram, a simulation was performed using a simulator that used a combination of the Butler-Volmer and diffusion equations[27]. The fitting results are shown in Supplementary Figs. 3–16. It is important to note that to perform quantitative electrochemical analysis of the mitochondrial respiratory chain, the electron transfer frequency (ETF) was adopted in this study as the current value j divided by the number of active sites of the enzyme. The unit of the ETF is e^- $site^{-1}$ s^{-1}, which facilitates the analysis of the oxygen consumption rate per active site of the enzyme. The values of j_0 and ETF_0 are shown in Supplementary Table 3; j_0 (10^{-7}–10^{-10} A cm^{-2}) and ETF_0 (10^{-7}–10^{-2} e^- $site^{-1}$ s^{-1}) in complex IV were quite small compared with those of the other complexes. The electrochemical exchange current refers to the activity of the electrode catalyst and quantitatively depends on the activation energy of the catalytic reaction. Therefore, the small exchange current value of complex IV indicates that the overpotential is large and that the driving force of the redox reactions in the respiratory chain system is largely complex IV.

Since the exchange current value ETF_0 per active site has been determined, the relationship between ETF and η for each enzyme has been found. Once the ETF is determined, η for each enzyme can be determined. Thus, we estimated the typical ETF values for mitochondrial respiration from the literature. Supplementary Table 1 lists the average oxygen consumption data of the cells obtained from the literature[28]. This oxygen consumption was divided by the number of complex IV molecules contained in each cell (Supplementary Table 2), and the reaction rate per complex IV molecule was converted to the electron transfer rate per unit time or ETF. Supplementary Figure 1 shows ETFs for various mitochondrial respiratory chains, which were distributed at 1-10 e^- $site^{-1}$ s^{-1}. Details of the method used to calculate the oxygen consumption rate are provided in the Supplementary Material.

Assuming a reaction circuit consisting of complexes I, III, and IV of the mitochondrial respiratory chain (Fig. 1d) and a typical ETF of 1-10 e^- $site^{-1}$ s^{-1}, we estimated the overpotential and thermogenesis of the entire circuit. Figure 1d can be regarded as a series circuit; therefore, the steady-state current values flowing through each enzyme in complexes I, III, and IV are equal, and the sum of these overpotentials is the overpotential of the entire circuit. Figure 2a shows the reaction overpotential and the sum of overpotentials for each enzyme at ETF = 4 e^- $site^{-1}$ s^{-1}. As relatively large overpotentials, 0.4 ± 0.1 V is used for the oxygen reduction reaction of complex IV, and 0.2 ± 0.1 V is used for the ubiquinone reduction of complex I. The sum of the overpotentials is approximately 0.60 V. That is, approximately 54% of the net energy of the respiratory chain (1.1 V) is used as the overpotential to drive the reaction, which is ultimately converted to heat. Figure 2b shows the relationship between ETF and total overpotential. This relationship is a function of the Butler-Volmer equation; however, as the ETF increases, the overpotential and the proportion of thermogenesis to total energy also increase. An important finding of this study is that the rate of thermogenesis increases with increasing oxygen consumption.

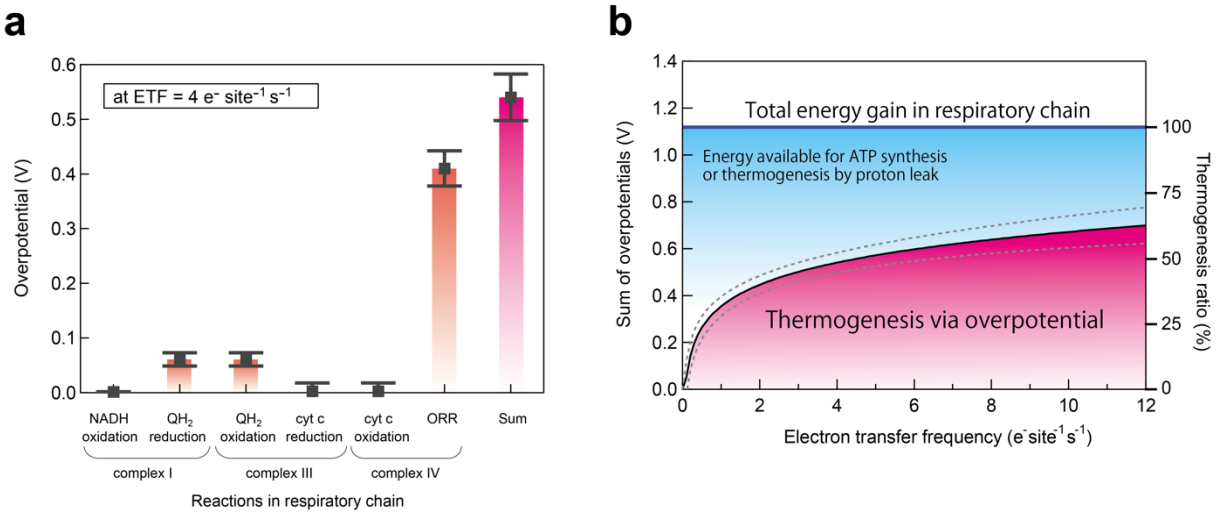

Fig. 2 | Estimated overpotentials and thermogenesis in a mitochondrial respiratoy chain. **a**, Calculated overpotential in each reaction at respiration activity of 4 e^- $site^{-1}$ s^{-1} for NADH oxidation in complex I, ubiquinone reduction in complex I, ubiquinol oxidation in complex III, cytochrome c reduction in complex III, cytochrome c oxidation in complex IV, and oxygen Reduction Reaction (ORR) in complex IV. **b**, Estimated total overpotential applied in a respiratory chain as a function of respiration activity. The dotted lines reflect the error bqr in **a**.

The first important result shown in Figure 2 is that the proportion of thermogenesis in the total respiratory chain energy gain, 39–63 % (ETF = 1-10 e^- $site^{-1}$ s^{-1}), estimated in the present study is in good agreement with the literature data of 40–60%[13,14] (see the example of values for various cells in Supplementary Fig. 2). That is, the remaining 37–61 % of the Gibbs free energy change in ORR becomes available energy for ATP synthesis. Second, it was clearly shown that the amount of heat produced changed depending on the oxygen consumption rate corresponding to the ETF. It was also quantitatively demonstrated that the rate of thermogenesis increased with oxygen consumption rate. Thirdly, thermogenesis occurred mostly (more than 70%) in complex IV. Identification of heat spots is important for future molecular research on mitochondria. Fourth, it was suggested that thermogenesis due to proton transfer was negligible. In this study, we assumed that the resistance to proton transfer was zero, and that the work gained by proton pumping was equal to the energy required for ATP synthesis, that is, the assumption of zero activation energy for proton pumping. The fact that thermogenesis due to enzymatic reactions matches the actual thermogenesis indicates that this assumption is correct. Although the activation energy required for proton transfer is finite and thermogenesis is not zero, it is considered to be much smaller than the activation energy of the reactions in the respiratory chain. It should be noted that the work obtained by proton transfer and the activation energy required for proton transfer have different meanings: the former is an equilibrium value and the latter is a non-equilibrium value.

Based on the results shown in Fig. 2, we estimated the distribution of work gained by the proton pumps and energy loss as thermogenesis in complexes I, III, and IV. Figure 3 shows the polarization curves of each enzyme reaction in complexes I, III, and IV plotted against the potential. The standard redox potential, exchange current density, and Tafel slope used for each

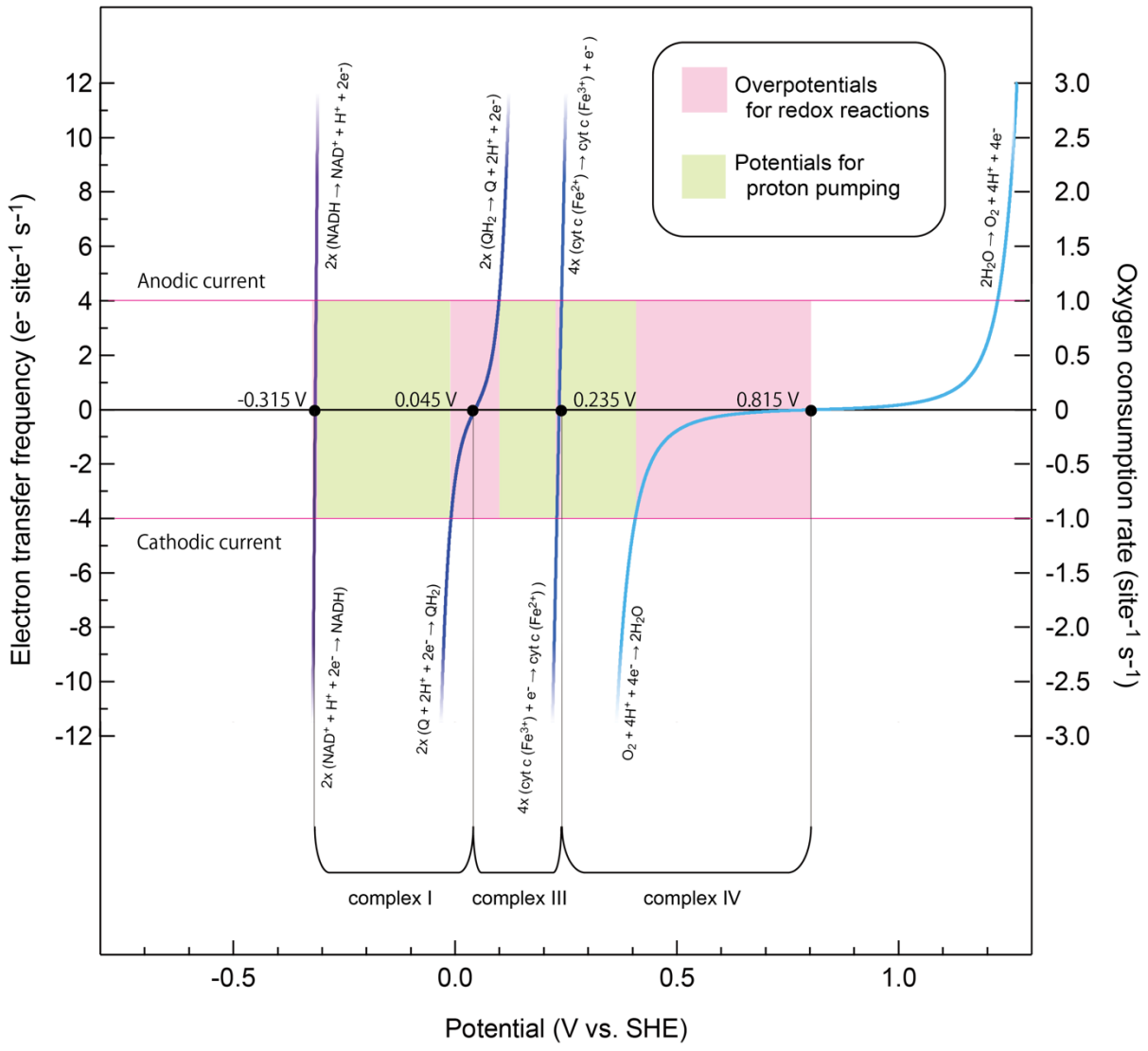

Fig. 3. | Electrochemical energy partitioning in a respiratory chain. Polarization curves of each enzymatic reaction in complex I, III, and IV based on kinetic parameters estimated in the present study. The pink and light green areas correspond to the power used for overpotential followed by heat dissipation and for proton pumping for ATP synthesis, respectively.

polarization curve were the average values listed in Supplementary Table 3. The positive current is the anode current resulting from an oxidation reaction, and the negative current is the cathode current resulting from a reduction reaction. In the steady state, the anode and cathode currents have the same magnitude but opposite signs. For example, $NADH \rightarrow NAD^+ + H^+ + 2e^-$ in complex I corresponds to an anodic reaction, wherein a positive current flows in the polarization curve. On the other hand, $Q + 2H^+ + 2e^- \rightarrow QH_2$ in complex I is a cathodic reaction and corresponds to a negative current. In Fig. 3, the thermogenesis due to overpotential when

ETF = 4 e^- $site^{-1}s^{-1}$ is marked in pink, and the work gained by the proton pump or ATP production is marked in yellow-green. It can be observed that heat is not significantly produced in complexes I and III, and the heat part is about 20 % compared with the sum of driving forces (0.235 V – (–0.315 V) = 0.55 V). In complex IV, on the other hand, the heat part was about 80%, indicating that most of the heat was produced in complex IV. Looking at the total area, the pink and yellow-green parts were almost the same, about 50 %. That is, when ETF = 4 e^- $site^{-1}$ s^{-1}, 50% of the energy gain of the respiratory chain reaction is used for overpotential or thermogenesis, and 50% is available for ATP production. More interestingly, Figure 3 explains the literature values for the proton transfer numbers in complexes I, III, and IV. It is believed that the proton transfers over the 0.15 V intermembrane potential difference. The energy gain for proton pumping (pink part) was shown to be approximately 0.3 eV, 0.12 eV, and 0.12 eV for complexes I, III, and IV, respectively. Therefore, the energy required to pump one proton was approximately 0.15 eV. ETF = 4 e^- $site^{-1}$ s^{-1} means that a four-electron process occurs once, $O_2 + 4\ H^+ + 4\ e^- \rightarrow 2\ H_2O$, which means that one oxygen molecule is consumed in the respiratory chain. Therefore, it is possible to do work four times the potential difference in the yellow part. In other words, each time one oxygen molecule is consumed, work of 1.2 eV, 0.48 eV, and 0.48 eV is done in respiratory chains I, III, and IV, respectively, corresponding to 8, 3.2, and 3.2 protons transported through the membrane. These numbers of protons are close to those reported in the literature. However, these numbers varied slightly depending on the respiration rate.

In this study, we propose an overpotential-derived thermogenesis model in which the Gibbs free energy change of NADH oxidation through aerobic respiration is used to drive the reaction of the respiratory chain and is then dissipated as heat. The kinetic parameters of the enzymatic reactions in the respiratory chain were analyzed using previously reported data, and the sum of the overpotentials in a series circuit of the respiratory chain was quantitatively estimated. As a result, the ratio of thermogenesis to total energy was 39-63 %, which is consistent with literature values. We also found a relationship between the rate of oxygen consumption, the rate of thermogenesis, and the division of energy used for thermogenesis and proton pumping in each complex. The above results indicate that the function of the respiratory chain in mitochondria can be analyzed in detail, and it is expected that the mechanism of respiratory function will be further elucidated from the perspective of chemical reactions in the future.

Reference

1. Bertholet, A. M. *et al.* H^+ transport is an integral function of the mitochondrial ADP/ATP carrier. *Nature* **571**, 515–520 (2019).
2. Bertholet, A. M. *et al.* Mitochondrial uncouplers induce proton leak by activating AAC and UCP1. *Nature* **606**, 180–187 (2022).
3. Kiyonaka, S. *et al.* Validating subcellular thermal changes revealed by fluorescent thermosensors. *Nat Methods* **12**, 801–802 (2015).
4. Lowell, B. B. & Spiegelman, B. M. Towards a molecular understanding of adaptive thermogenesis. *Nature* **404**, 652–660 (2000).
5. Chouchani, E. T., Kazak, L. & Spiegelman, B. M. New Advances in Adaptive Thermogenesis: UCP1 and Beyond. *Cell Metab* **29**, 27–37 (2019).
6. Bertholet, A. M. *et al.* Mitochondrial uncouplers induce proton leak by activating AAC and UCP1. *Nature* **606**, 180–187 (2022).
7. Bertholet, A. M. & Kirichok, Y. The mechanism FA-dependent H+ transport by UCP1. *Handb Exp Pharmacol* **251**, 143–159 (2019).

8. Bockris, M., Gutmann, F. & Habib, M. A. *A Fuel Cell Model in Biological Energy Conversion*. *Journal of Biological Physics* vol. 13 (1985).
9. Bockris, J. Predominantly Electrochemical Nature of Biological Power-producing Reactions. *Nature* **215**, 197 (1967).
10. Berry, M. N., Grivell, A. R. & Wallace, P. G. *Electrochemical Aspects of Metabolism*.
11. Mitchell, P. Coupling of Phosphorylation to Electron and Hydrogen Transfer by a Chemi-Osmotic type of Mechanism. *Nature* **191**, 144–148 (1961).
12. Mitchell, P. Chemiosmotic coupling in oxidative and photosynthetic phosphorylation. *Biochimica et Biophysica Acta - Bioenergetics* vol. 1807 1507–1538 Preprint at https://doi.org/10.1016/j.bbabio.2011.09.018 (2011).
13. Macherel, D., Haraux, F., Guillou, H. & Bourgeois, O. The conundrum of hot mitochondria. *Biochim Biophys Acta Bioenerg* **1862**, (2021).
14. Nath, S. The thermodynamic efficiency of ATP synthesis in oxidative phosphorylation. *Biophys Chem* **219**, 69–74 (2016).
15. Barker, C. D., Reda, T. & Hirst, J. The flavoprotein subcomplex of complex I (NADH:ubiquinone oxidoreductase) from bovine heart mitochondria: Insights into the mechanisms of NADH oxidation and NAD+ reduction from protein film voltammetry. *Biochemistry* **46**, 3454–3464 (2007).
16. Srinivas, S., Ashokkumar, K., Sriraghavan, K. & Senthil Kumar, A. A prototype device of microliter volume voltammetric pH sensor based on carbazole-quinone redox-probe tethered MWCNT modified three-in-one screen-printed electrode. *Sci Rep* **11**, 13905 (2021).
17. Arthisree, D. *et al.* A hydrophobic coenzyme Q10 stabilized functionalized-MWCNT modified electrode as an efficient functional biomimetic system for the electron-transfer study. *Colloids Surf A Physicochem Eng Asp* **504**, 53–61 (2016).
18. Gandhi, M., Rajagopal, D. & Senthil Kumar, A. Molecularly wiring of Cytochrome c with carboxylic acid functionalized hydroquinone on MWCNT surface and its bioelectrocatalytic reduction of H2O2 relevance to biomimetic electron-transport and redox signalling. *Electrochim Acta* **368**, (2021).
19. Ray, S., Yadav, D., Garje, S. S. & Mazumdar, S. Transition metal complexes as promoters of direct electron transfer from gold electrodes to cytochrome c. *J.Chem.Schi* (2021) doi:10.1007/s12039-021.
20. Lebègue, E. *et al.* An optimal surface concentration of pure cardiolipin deposited onto glassy carbon electrode promoting the direct electron transfer of cytochrome-c. *Journal of Electroanalytical Chemistry* **808**, 286–292 (2018).
21. Chatterjee, S., Sengupta, K., Hematian, S., Karlin, K. D. & Dey, A. Electrocatalytic O2-reduction by synthetic cytochrome c oxidase mimics: Identification of a 'bridging peroxo' intermediate involved in facile 4e-/4H+ O2-reduction. *J Am Chem Soc* **137**, 12897–12905 (2015).
22. Mukherjee, S. *et al.* A biosynthetic model of cytochrome c oxidase as an electrocatalyst for oxygen reduction. *Nat Commun* **6**, (2015).
23. Bhunia, S. *et al.* Rational Design of Mononuclear Iron Porphyrins for Facile and Selective 4e-/4H+ O2 Reduction: Activation of O-O Bond by 2nd Sphere Hydrogen Bonding. *J Am Chem Soc* **140**, 9444–9457 (2018).
24. Du, C. *et al.* A Cu and Fe dual-atom nanozyme mimicking cytochrome c oxidase to boost the oxygen reduction reaction. *J Mater Chem A Mater* **8**, 16994–17001 (2020).
25. Zhang, H. *et al.* Bionic design of cytochrome c oxidase-like single-atom nanozymes for oxygen reduction reaction in enzymatic biofuel cells. *Nano Energy* **83**, (2021).
26. Xu, C. *et al.* Contracted Fe–N 5 –C 11 Sites in Single-Atom Catalysts Boosting Catalytic Performance for Oxygen Reduction Reaction . *ACS Appl Mater Interfaces* (2023) doi:10.1021/acsami.3c03982.
27. Brown, J. H. Development and Use of a Cyclic Voltammetry Simulator To Introduce Undergraduate Students to Electrochemical Simulations. *J Chem Educ* **92**, 1490–1496 (2015).
28. Wagner, B. A., Venkataraman, S. & Buettner, G. R. The rate of oxygen utilization by cells. *Free Radic Biol Med* **51**, 700–712 (2011).

Funding:

This work was supported by a JSPS Grant-in-Aid for Scientific Research (KAKENHI) Grant Number 23H05459, JST establishment of university fellowships for the creation of science technology innovation Grant Number JPMJFS2106, and the TRiSTAR Program, a Top Runner Development Program Engaging Universities, National Labs, and Companies. K.T. acknowledges Dr. Naohito Otani, Mr. Kennichi Kazama, Mr. Yuichi Enomoto, and Dr. Satoshi Harashima for fruitful discussions and funding aid through Academist crowdfunding.

Author contribution

Author contributions: J.N. conceived thermogenesis by overpotential. K.T. conceived an electrochemical circuit model for the respiratory chain. J.N. and K.T. designed analytical protocols. N.A.P.N. performed the analyses and the calculations. N.A.P.N., M.Y., J.N. and K.T. discussed the results and prepared the manuscript for publication.

Competing interests: The authors declare no conflict of interest.